

Missense Mutations of the Pro65 Residue of PCGF2 Cause a Recognizable Syndrome Associated with Craniofacial, Neurological, Cardiovascular, and Skeletal Features

Peter D. Turnpenny,^{1,28,*} Michael J. Wright,² Melissa Sloman,³ Richard Caswell,⁴ Anthony J. van Essen,^{5,29} Erica Gerkes,⁵ Rolph Pfundt,⁶ Susan M. White,^{7,8} Nava Shaul-Lotan,⁹ Lori Carpenter,¹⁰ G. Bradley Schaefer,¹¹ Alan Fryer,¹² A. Micheil Innes,¹³ Kirsten P. Forbes,¹⁴ Wendy K. Chung,¹⁵ Heather McLaughlin,¹⁶ Lindsay B. Henderson,¹⁶ Amy E. Roberts,¹⁷ Karen E. Heath,^{18,19} Beatriz Paumard-Hernández,^{18,19} Blanca Gener,^{19,20} the DDD study,²¹ Katherine A. Fawcett,^{22,27} Romana Gjergja-Juraški,²³ Daniela T. Pilz,²⁴ and Andrew E. Fry^{25,26,28,*}

PCGF2 encodes the polycomb group ring finger 2 protein, a transcriptional repressor involved in cell proliferation, differentiation, and embryogenesis. *PCGF2* is a component of the polycomb repressive complex 1 (PRC1), a multiprotein complex which controls gene silencing through histone modification and chromatin remodelling. We report the phenotypic characterization of 13 patients (11 unrelated individuals and a pair of monozygotic twins) with missense mutations in *PCGF2*. All the mutations affected the same highly conserved proline in *PCGF2* and were *de novo*, excepting maternal mosaicism in one. The patients demonstrated a recognizable facial gestalt, intellectual disability, feeding problems, impaired growth, and a range of brain, cardiovascular, and skeletal abnormalities. Computer structural modeling suggests the substitutions alter an N-terminal loop of *PCGF2* critical for histone binding. Mutant *PCGF2* may have dominant-negative effects, sequestering PRC1 components into complexes that lack the ability to interact efficiently with histones. These findings demonstrate the important role of *PCGF2* in human development and confirm that heterozygous substitutions of the Pro65 residue of *PCGF2* cause a recognizable syndrome characterized by distinctive craniofacial, neurological, cardiovascular, and skeletal features.

PCGF2 [MIM 600346] encodes the polycomb group ring finger 2 protein (*PCGF2*, *aka* MEL18). The *PCGF2* protein contains an N-terminal RING finger motif and is similar in structure to other polycomb-group (PcG) proteins.¹ *PCGF2* has been implicated in cell proliferation,² X inactivation,³ regulation of homeobox genes during embryogenesis,⁴ mesoderm differentiation,⁵ hemopoiesis,⁶ tumor suppression,^{7,8} and angiogenesis.^{9,10} *PCGF2* is widely expressed in human tissues.^{1,11} It binds to a specific DNA sequence (5'-GACTNGACT-3') in the promoter regions of target genes.⁷ *PCGF2* is a component of a

multiprotein complex called the polycomb repressive complex 1 (PRC1), an essential regulator, via histone modification and chromatin remodeling, of transcription in embryonic and adult stem cells.^{12,13} The core of mammalian PRC1 typically contains an E3 ubiquitin ligase (RING1A [MIM 602045] or RING1B [MIM 608985]),^{3,14} that ubiquitinates histone H2A at lysine 119, along with a PCGF protein (*PCGF1-6*),¹⁵ which regulates the enzyme activity of the complex. PRC1 complexes often include other PcG components (e.g., polyhomeotic homolog or chromobox homolog proteins),

¹Peninsula Clinical Genetics, Royal Devon and Exeter NHS Foundation Trust, Exeter EX1 2ED, UK; ²Northern Genetics Service, Newcastle-upon-Tyne Hospitals NHS Foundation Trust, Newcastle NE1 3BZ, UK; ³Department of Molecular Genetics, Royal Devon and Exeter NHS Foundation Trust, Exeter EX2 5DW, UK; ⁴Institute of Biomedical and Clinical Science, University of Exeter Medical School, Exeter EX1 2LU, UK; ⁵Department of Genetics, University of Groningen, University Medical Center Groningen, 9700 RB Groningen, the Netherlands; ⁶Human Genetics, Radboud University Nijmegen Medical Centre, 6525 GA Nijmegen, the Netherlands; ⁷Victorian Clinical Genetics Services, Murdoch Children's Research Institute, Parkville, Victoria 3052, Australia; ⁸Department of Paediatrics, University of Melbourne, Parkville, Victoria 3052, Australia; ⁹Clinical Genetics, Hadassah-Hebrew University Medical Center, Ein Kerem, Jerusalem 91120, Israel; ¹⁰Saint Francis Genetics, Tulsa, Oklahoma 74136, USA; ¹¹University of Arkansas for Medical Sciences, Little Rock, Arkansas 72205, USA; ¹²Cheshire and Merseyside Clinical Genetic Service, Liverpool Women's NHS Foundation Trust, Liverpool L8 7SS, UK; ¹³Department of Medical Genetics and Alberta Children's Hospital Research Institute, Cumming School of Medicine, University of Calgary, Calgary, Alberta T3B 6A8, Canada; ¹⁴Department of Neuroradiology, Queen Elizabeth University Hospital, Glasgow G51 4TF, UK; ¹⁵Departments of Pediatrics and Medicine, Columbia University, New York, NY 10032, USA; ¹⁶GeneDx, Gaithersburg, Maryland 20877, USA; ¹⁷Cardiovascular Genetics, Department of Cardiology and Division of Genetics, Department of Medicine, Boston Children's Hospital, Boston, Massachusetts 02115, USA; ¹⁸Institute of Medical & Molecular Genetics (INGEMM) and Skeletal Dysplasia Multidisciplinary Unit (UMDE), Hospital Universitario la Paz, Universidad Autónoma de Madrid, IdiPAZ, 28046 Madrid, Spain; ¹⁹Centro de Investigación Biomédica en Red Enfermedades Raras (CIBERER), Instituto de Salud Carlos III (ISCIII), 28029 Madrid, Spain; ²⁰Department of Genetics, Cruces University Hospital, Biocruces Health Research Institute, 48903 Barakaldo, Bizkaia, Spain; ²¹Wellcome Trust Sanger Institute, Hinxton, Cambridge CB10 1SA, UK; ²²MRC Computational Genomics Analysis and Training Programme (CGAT), MRC Centre for Computational Biology, MRC Weatherall Institute of Molecular Medicine, John Radcliffe Hospital, Headington, Oxford OX3 9DS, UK; ²³Medical School of Osijek, Josip Juraj Strossmayer University, Neuropediatric Unit, Children's Hospital Srebrnjak, CRO-10000 Zagreb, Croatia; ²⁴West of Scotland Genetic Services, Queen Elizabeth University Hospital, Glasgow G51 4TF, UK; ²⁵Institute of Medical Genetics, University Hospital of Wales, Cardiff CF14 4XW, UK; ²⁶Division of Cancer and Genetics, School of Medicine, Cardiff University, Cardiff CF14 4XN, UK

²⁷Present address: Department of Health Sciences, University of Leicester, George Davies Centre, University Road, Leicester LE1 7RH, UK

²⁸These authors contributed equally to this work

²⁹Deceased

*Correspondence: peter.turnpenny@nhs.net (P.D.T.), fryae@cardiff.ac.uk (A.E.F.)

<https://doi.org/10.1016/j.ajhg.2018.09.012>

© 2018 American Society of Human Genetics.

which guide recruitment of PRC1 to the chromatin.¹² The variable composition of PRC1 allows the complex to modulate function depending on cell type and developmental stage. A range of other proteins involved in histone H2A ubiquitination have been linked to neurodevelopmental disorders.¹⁶ These include proteins involved in both adding^{17–19} and removing^{20–22} ubiquitin from H2A. Here, we report that mutations in *PCGF2* cause a recognizable developmental disorder.

Individuals 1 and 2 underwent exome sequencing as part of the Deciphering Developmental Disorders (DDD) study.²³ Both individuals had the same *de novo* missense mutation in *PCGF2*, c.194C>T, p.(Pro65Leu), and strikingly similar facial appearances. Identification of additional subjects with *PCGF2* variants was achieved through contact with other institutions and via GeneMatcher.²⁴ Thus, nine further unrelated individuals and a pair of monozygotic twin sisters with missense mutations in *PCGF2* were ascertained. The unrelated individuals all had the same mutation, c.194C>T, p.(Pro65Leu). The twin sisters (individuals 3 and 4) had a different mutation at the same residue, c.193C>T, p.(Pro65Ser). All mutations were *de novo*, apart from individual 11 whose asymptomatic mother was found to be mosaic (21% in blood DNA). Most mutations were identified by trio exome sequencing. Individual 6 was ascertained based on clinical features and the diagnosis confirmed by targeted Sanger sequencing.

To delineate the phenotypic spectrum associated with *PCGF2* mutations we collected detailed clinical information. Consent for publication of photographs was sought from the individuals' parents or legal guardians (Individual 13's parents did grant use of non-facial photographs - they are in Figure S2). Individuals who had evaluation or analysis beyond routine clinical care were part of research studies approved by either the Cambridge South Research Ethics Committee (10/H0305/83) or the Research Ethics Committee for Wales (09/MRE09/51). Detailed case reports for all the subjects are given in the Supplemental Note. Detailed molecular and clinical features for each individual are included in Table S1. Coding and protein positions for *PCGF2* are based on GenBank accession codes NM_007144.2 (ENST00000360797.2) and NP_009075.1, respectively.

The 13 subjects (7 females and 6 males) ranged in age from 2 to 21 years. The individuals all had similar distinctive facial features, intellectual disability, and impaired growth (Table S1). Clinical images from 12 of the subjects are shown in Figures 1, S1 and S2. Consistent facial features included a broad forehead with frontal bossing (13/13); sparse, slow growing hair, particularly in the frontal and temporal regions (12/12); peri-orbital fullness (12/12); and malar hypoplasia (12/12). The subjects' ears were dysplastic (12/12), typically with a satyr configuration, and often small and low set. Mild facial hypotonia was common. This impaired articulation of speech and led to an open mouth posture and

drooling (3/13). Patients often had short palpebral fissures (11/12) and/or oral aperture (7/12). A prominent nasal tip (10/13) and mandibular prognathism (7/13) were common in older individuals. The combination of large forehead, prominent jaw and open mouth results in the face often appearing long (7/12). The InterFace software package²⁵ was used to generate a composite average face (Figure S2).

The intellectual disability and/or developmental delay in the subjects ranged from mild to severe. Most individuals had difficulties with verbal communication. Three had absent speech at the time of assessment (at 21 years, 9 years, and 30 months of age). Muscular hypotonia (9/13) and conductive hearing impairment (7/13) were common. Only two subjects had a history of confirmed seizures. MRI brain scans for eight individuals were available for review (Figure 2). Mild enlargement of the lateral ventricles was common. Polymicrogyria, a malformation of cortical development, was noted in four individuals (bilateral extensive polymicrogyria in the twins, and bilateral perisylvian polymicrogyria in individuals 6 and 12). An irregular gyral pattern was reported in individual 9 but the MRI was not available for review. Patchy to confluent white matter changes were present in all reviewed scans, most prominently around the atria of the lateral ventricles. The white matter changes varied in severity and were most marked in the individuals with polymicrogyria. In some areas the abnormal white matter had the appearance of prominent perivascular spaces. Individual 1 reportedly had a thin corpus callosum. Individual 9 was reported to have mild cerebellar vermis hypoplasia. MR angiography was performed in three individuals. This showed a variable degree of tortuosity and ectasia of the intra- and extracranial blood vessels. Tortuous retinal vessels were reported in individual 7.

Intrauterine growth restriction was noted during three pregnancies (borderline in one more). All the subjects had a birth weight below the mean for gestational age. Weight during childhood remained low, compounded by feeding difficulties (9/13) and/or gastroesophageal reflux (6/13). The feeding problems and reflux improved slowly with age. Constipation was also common (8/12), sometimes severe. Height during childhood was generally low for age although three subjects had heights just above the mean. The effects on head size were variable. Individual 1, the oldest and most intellectually impaired individual in the group, had a relatively large head size from early childhood, originally attributed to arrested hydrocephalus (occipitofrontal circumference [OFC] +1.8 SD, height and weight 1–2 SD below the mean). Relative macrocephaly was noted in two other individuals. In contrast, four individuals had small heads (OFC < –2 SD). Eleven subjects had cardiac abnormalities. Findings included patent ductus arteriosus (PDA) (5/13), atrial septal defect (3/13), and dilatation of the ascending aorta (5/13). Individual 5 had a PDA and prolapse of both mitral and tricuspid valves with some regurgitation. Individual 10 had aortic dilatation and an episode of supraventricular

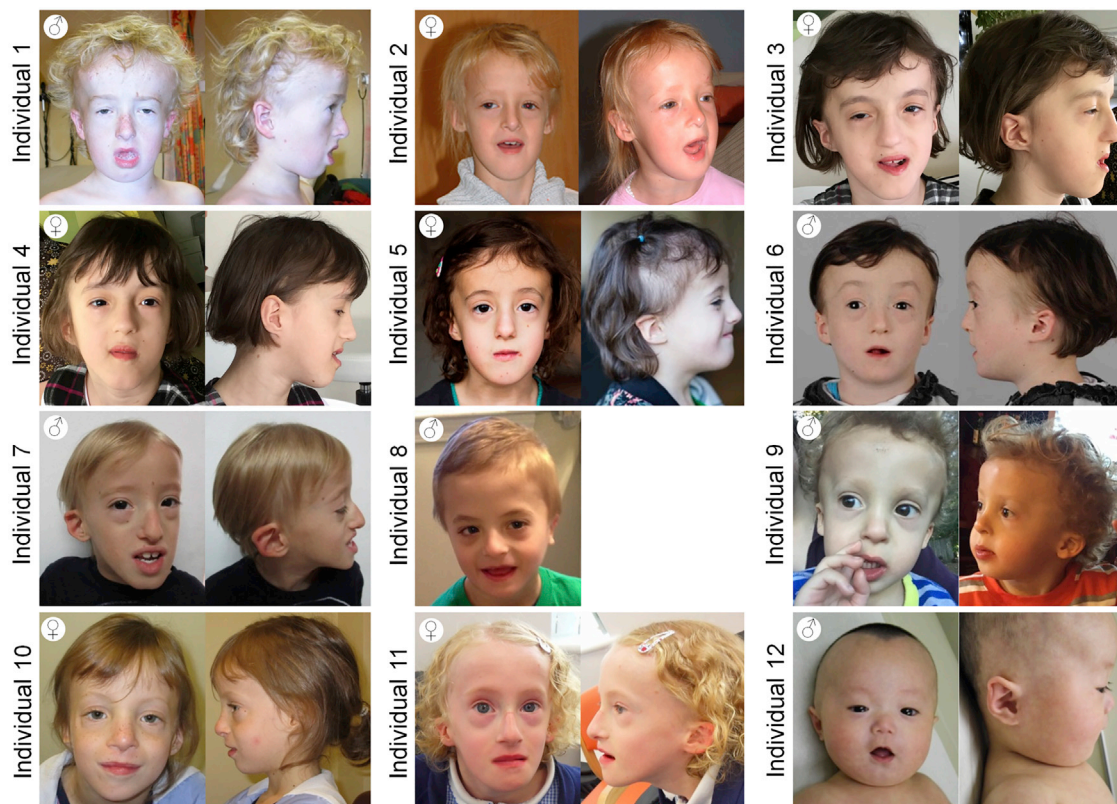


Figure 1. Facial Features of Individuals with *PCGF2* Mutations

Each individual is noted with the corresponding number used throughout the manuscript. Included on the top left of each cluster is the sex. Ages are: individual 1, 12 years; individual 2, 8.5 years; individual 3, 8 years; individual 4, 8 years; individual 5, 7 years (left), 4 years (right); individual 6, 9 years; individual 7, 7 years; individual 8, 6 years; individual 9, 2 years (left), 3 years (right); individual 10, 9 years; individual 11, 8 years; individual 12, 3 months. Consistent facial features include a broad forehead, long face, malar hypoplasia, small mouth, small palpebral fissures, periorbital fullness, prominent nose (particularly in older individuals), and dysplastic, low-set ears.

tachycardia. Individual 1 was found to have a severely dilated aortic root at the age of 21 years (diameter 4.7 cm at the sinus of valsalva, Z score > 7). No arterial aneurysms or dissections were reported in the subjects. Skeletal anomalies were observed in several individuals. These included hypoplasia of the L1 vertebra (individual 1), small T3 vertebral body (individual 5), and a truncated sacrum (individual 6). Kyphosis and/or scoliosis (6/13), pectus deformities (3/13), and minor digital anomalies (4/13) were also found. Individual 1 had a skeletal survey at age 2.5 years, which revealed delayed epiphyseal ossification, particularly of the carpal bones, and pseudo-epiphyses of many metacarpal bones. Two cases (individuals 2 and 4) had a small diaphragmatic hernia of the Morgagni type.

The identified mutations all affected the Pro65 residue of *PCGF2*. This residue is located just after the N-terminal RING finger motif and is highly conserved across species and other human *PCGF* proteins (Figures 3A and 3B). No variants have been reported at this position in the gnomAD database in *PCGF2* or at the equivalent proline in other human *PCGF* proteins. Both mutations were predicted to be deleterious by a majority of *in silico* prediction programs (Table S1). To explore the effects of Pro65 muta-

tions, we modeled the structure of the N-terminal of *PCGF2* (amino acids 5-101) based on solved crystal structures for its homolog, BMI1 (*PCGF4*) [MIM 164831]. Two templates were used, PDB 2h0d (BMI1 bound to RING1B)²⁶ and PDB 4r8p (BMI1-PRC1 complex bound to nucleosome),²⁷ with essentially identical results. Pro65 is situated at the junction between an extended loop region and a short α -helix (Figure 3C). The presence of proline at this position is likely to maintain the transition from loop to helix. Furthermore, given the rotational constraint imposed by proline's ring structure, this residue is likely to provide the loop region with a degree of structural rigidity.²⁸ Thermodynamic analysis of the 2h0d-based *PCGF2* model using FoldX showed the Pro65 variants resulted in changes to thermodynamic stability ($\Delta\Delta G$) of +8.6 kcal/mol and +3.9 kcal/mol for p.Pro65Leu and p.Pro65Ser respectively; $\Delta\Delta G$ values > 3 kcal/mol are generally regarded as destabilizing.²⁹ Intriguingly, the loop region next to Pro65 contains two basic residues, Lys62 and Arg64, which form a basic patch on BMI1 and the predicted surface of *PCGF2* (Figures 3D and 3E). PRC1 complexes containing *PCGF2* (or BMI1) have low intrinsic ubiquitin ligase activity compared to complexes containing other *PCGF* proteins.³⁰ This is compensated

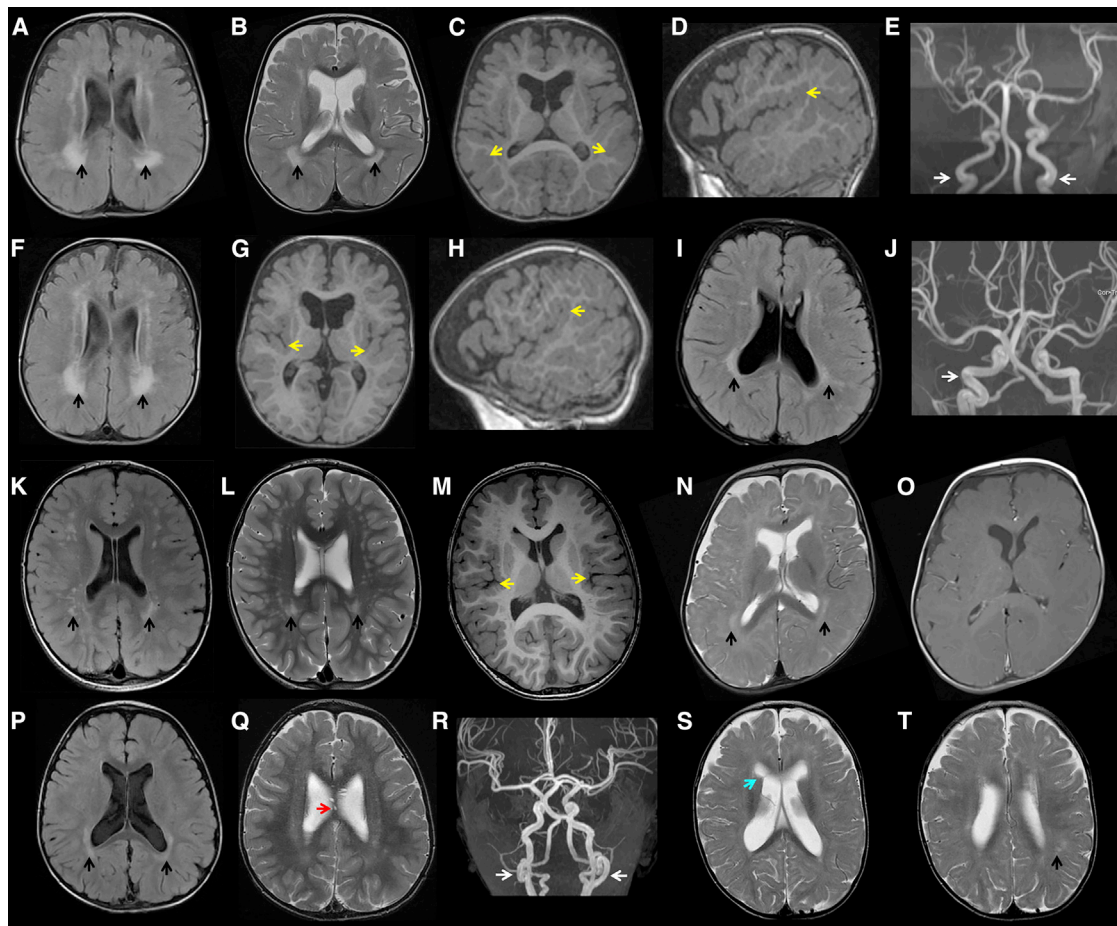


Figure 2. MRI Brain Abnormalities in Individuals with *PCGF2* Mutations

(A–E) Axial (FLAIR, T2 and T1), sagittal (T1), and MRA images from individual 3 at age 21 months.

(F–H) Axial (FLAIR and T1) and sagittal (T1) images from individual 4 at age 21 months.

(I and J) Axial FLAIR and MRA images from individual 5 at age 3 years and 3 months.

(K–M) Axial (FLAIR, T2 and T1) images from individual 6 at age 5 years.

(N and O) Axial (T2 and T1) images from individual 7 at age 10 months.

(P–R) Axial (FLAIR and T2) and MRA images from individual 8 at age 37 months.

(S and T) Axial T2 images from individual 10 at age 13 months.

The images show patchy white matter hyperintensity in the T2 and FLAIR images (black arrows). The patches are scattered throughout the white matter but are consistently seen in the peri-atrial region. Other findings included enlargement of the lateral ventricles; increased anterior extra-axial fluid spaces (e.g., B, G, N, and S); bilateral polymicrogyria (yellow arrows, subtle in M); prominence of the perivascular spaces, including in the corpus callosum (red arrow, Q); coarctation of the frontal horns (blue arrow, S). MRA showed tortuosity (white arrows) of the internal carotid (E), (J), and vertebral (R) arteries.

for by an increased affinity for the nucleosomal substrate, leading to efficient histone ubiquitination. The increased affinity is dependent on residues Lys62 and Arg64, which interact with an acidic patch on the surface of histones 3 and 4 (Figure 3F). This raises the possibility that the interaction between PCGF2 and histones is disrupted by the structural perturbations caused by Pro65 substitutions.

The extreme clustering of disease-causing *de novo* missense mutations in *PCGF2* is highly statistically significant and similar to other genes with non-haploinsufficient disease mechanisms.³¹ No truncating mutations were observed in our cohort. In contrast, several truncating *PCGF2* variants are listed by the gnomAD database. This argues against a simple haploinsufficiency mechanism. The probability of *PCGF2* being loss-of-function intolerant

(pLI)³² in the Exome Aggregation Consortium (ExAC) database is only 0.55. Furthermore, no interstitial deletions involving *PCGF2* are listed on the DECIPHER database. Loss of *PSc* (the homolog of *PCGF*) in *Drosophila melanogaster* leads to mis-expression of homeotic genes and defects in segmental determination.³³ Similarly, homozygote *Pcgf2*-deficient mice exhibit disturbed Hox gene expression with posterior transformations of the axial skeleton and growth retardation.⁴ However, heterozygous *Pcgf2*-deficient mice were normal, and no abnormalities of craniofacial structure or neurology were identified in the homozygotes. Our *in silico* structural modeling suggests substitution of Pro65 disrupts the interaction of PCGF2 with histones. This provides a plausible molecular mechanism for a dominant-negative effect. Mutant PCGF2 might

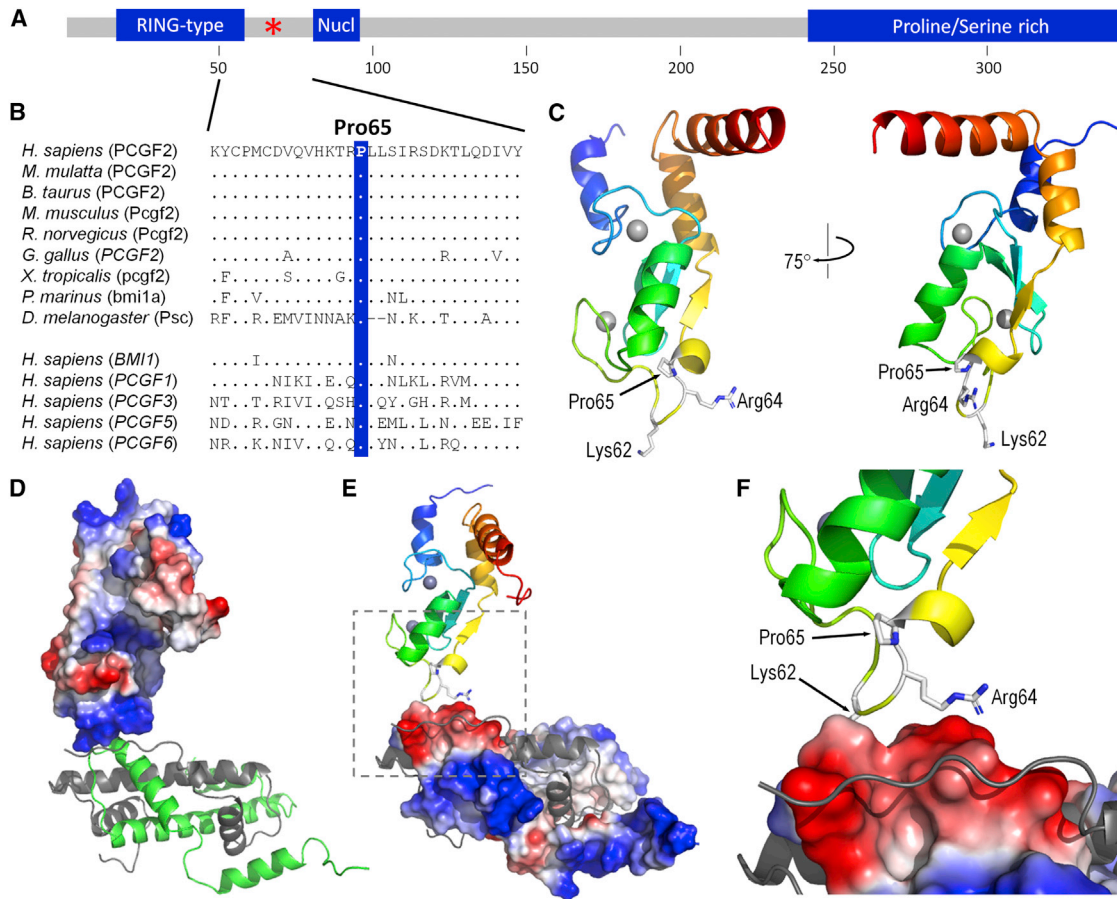


Figure 3. Localization of the PCGF2 Mutations

(A) Schematic domains of PCGF2. The domains and motifs of PCGF2 (UniprotKB: P35227) are illustrated. These include a RING-type Zinc finger (residues 18–57), nuclear localization signal (81–95) and Proline/Serine-rich domain (242–344). The location of the Pro65 residue is marked by the red asterisk. Residue number is indicated in the scale below the illustration.

(B) The PCGF2 mutations are located at the highly conserved Pro65 residue. ClustalW homology alignments for Human PCGF2 (residues 51–80) and a range of orthologs and paralogs. Orthologs include Human (NP_009075.1), Rhesus monkey (XP_001083817.1), Cow (NP_001137578.1), Mouse (NP_001156779.1), Rat (NP_001099306.1), Chicken (XP_003642857.1), Frog (NP_001025573.1), Lamprey (ENSPMAP00000007297.1), and Fruit fly (NP_523725.2). Paralogs include BMI1/PCGF4 (NP_005171.4), PCGF1 (NP_116062.2), PCGF3 (NP_006306.2), PCGF5 (NP_001243478.1), and PCGF6 (NP_001011663.1). Identical residues are indicated by dots. The blue bar highlights the position of the Pro65 residue.

(C) Structural model of human PCGF2 (residues 5–101, modeled on template 2h0d). Two views of the model are shown in ribbon format, colored from blue, N-terminal, to red, C-terminal, with side-chains shown for Pro65, Arg64, and Lys62. Grey spheres represent bound zinc ions; interaction with RING1B is primarily mediated via residues in helices 1 and 3 (blue and orange, respectively).

(D) The interaction between PCGF2 and histone H3/4 (modeled on template 4r8p). The predicted molecular surface of PCGF2 (left) is colored by electrostatic charge (blue, basic; red, acidic); histone chains from 4r8p are shown as green (H3.2) and gray (H4) ribbons, respectively; other chains of the complex have been omitted for clarity; note the basic patch of PCGF2 in contact with H3.2.

(E) As (D), but showing surface charge for H3.2, with PCGF2 shown as a ribbon colored from N-terminal, blue to C-terminal, red; note the acidic patch of H3.2 lying opposite the basic patch of PCGF2.

(F) As (E), but showing detail around the PCGF2/H3.2 interface; the regions shown are outlined by gray broken lines in part E; sidechains of PCGF2 Pro65, Arg64, and Lys62 (partially obscured) are shown in stick format.

retain the ability to sequester other PcG components into PRC1 complexes but, due to disruption of the loop structure around Lys62 and Arg64, mutant PRC1 complexes might lack the ability to interact efficiently with histones. Detailed functional experiments will be required to distinguish between these and other possible pathogenic mechanisms at a molecular level.

PCGF2 regulates differentiation of the cardiac mesoderm, which might contribute to the cardiac anomalies seen.⁵ Aortic dilation was found in five of the subjects (se-

vere in individual 1, the young adult). We would therefore recommend that all PCGF2 patients have periodic echocardiographic surveillance. The brain and vascular abnormalities seen in patients might be due to disturbed PI3K-AKT signaling, a critical pathway regulating growth, angiogenesis, and neural development. Loss of PCGF2 function leads to downregulation of PTEN [MIM 601728], promoting activation of AKT [MIM 164730], increased HIF-1 α [MIM 603348] levels, and expression of vascular endothelial growth factor [MIM 192240].¹⁰ In addition, PCGF2

binds directly to CCND2 [MIM 123833], a downstream effector of the PI3K-AKT pathway in developing neuroblasts.³⁴ Gain-of-function mutations in *CCND2* and other components of the PI3K-AKT pathway have been found to cause polymicrogyria, macrocephaly, and ventricular dilation.^{35,36} Knockdown of *PCGF2* has been shown to increase proliferative activity in cells overexpressing *CCND2*.³⁴ If Pro65 mutations reduce *PCGF2*'s ability to inhibit *CCND2*, the increased *CCND2* activity may predispose to polymicrogyria. The *CCND2* binding site has been mapped to the C-terminal proline/serine-rich domain of *PCGF2*.³⁴ Therefore, mutation of the N-terminal Pro65 residue is unlikely to directly block binding of *CCND2*. The presence of vascular abnormalities (and the twin placental circulation of individuals 3 and 4) may be additional risk factors for the polymicrogyria.³⁷ The variable head size observed in subjects may reflect the conflicting effects of abnormal vasculature (impairing brain growth and causing the deep cerebral white matter changes) and altered signaling through the PI3K-AKT-*CCND2* pathway (promoting brain growth and ventricular dilation). *PCGF2* has tumor suppression activity and has been implicated in a range of tumor types.^{7,38–40} To date, none of the subjects with *PCGF2* Pro65 mutations has been diagnosed with malignancy.

In summary, we have reported 13 individuals with missense substitutions of the Pro65 residue of *PCGF2*. These individuals have a recognizable phenotype of developmental delay, intellectual disability, impaired growth, and characteristic facial features that include frontal bossing, sparse hair, malar hypoplasia, small palpebral fissures and oral stoma, and dysplastic “satyr” ears. Other common findings in the subjects included feeding problems, constipation, and a range of brain, cardiac, vascular, and skeletal malformations. Further work is required to define the precise pathogenic mechanism of *PCGF2* mutations; however, our modeling and the available genetic data suggests that *PCGF2* Pro65 mutations have dominant-negative effects on PRC1 function, altering multiple signaling pathways and therefore resulting in the complex human phenotype.

Supplemental Data

Supplemental data include two figures, one table, and a Supplemental Note and can be found with this article online at <https://doi.org/10.1016/j.ajhg.2018.09.012>.

Acknowledgments

We thank the individuals and their families for their willingness to participate in this study. We are grateful to Caroline Wright (Exeter) for her comments on the manuscript and to Bert de Vries (Nijmegen), Orly Elpeleg (Jerusalem), and Megan Cho (GeneDx) for alerting us to new cases that would not otherwise have been part of this collaboration.

A.E.F. was supported by the Academy of Medical Sciences (grant: AMS-SGCL8-Fry). This work was also supported by the Wales Epilepsy Research Network and the Wales Gene Park.

W.K.C. received support from the Simons Foundation and JPB Foundation. K.E.H. received support from MINECO (grants: SAF2015-66831-R, SAF2017-84646-R). The DDD study presents independent research commissioned by the Health Innovation Challenge Fund (grant number HICF-1009-003), a parallel funding partnership between the Wellcome Trust and the Department of Health, and the Wellcome Trust Sanger Institute (grant number WT098051). The views expressed in this publication are those of the author(s) and not necessarily those of the funding agencies.

Declaration of Interests

H.M. and L.B.H. are employees of GeneDx, Inc., a wholly owned subsidiary of OPKO Health, Inc. The other authors declare no competing interests.

Received: May 16, 2018

Accepted: September 22, 2018

Published: October 18, 2018

Web Resources

CADD, <https://cadd.gs.washington.edu/>
Deciphering Developmental Disorders, <http://www.ddduk.org/>
DECIPHER, <https://decipher.sanger.ac.uk/>
ExAC Browser, <http://exac.broadinstitute.org/>
FoldX, <http://foldxsuite.crg.eu/>
GenBank, <https://www.ncbi.nlm.nih.gov/genbank/>
GeneMatcher, <https://genematcher.org/>
gnomAD Browser, <http://gnomad.broadinstitute.org/>
InterFace Software Package, <https://www.york.ac.uk/psychology/interface/>
MutationTaster, <http://www.mutationtaster.org/>
OMIM, <http://www.omim.org/>
PolyPhen-2, <http://genetics.bwh.harvard.edu/pph2/>
RCSB Protein Data Bank, <http://www.rcsb.org/pdb/home/home.do>
SIFT, <http://sift.bii.a-star.edu.sg/>
SMART, <http://www.smart.embl-heidelberg.de/>
The Human Protein Atlas, <http://www.proteinatlas.org/>
SWISS-MODEL, <http://swissmodel.expasy.org/>
UCSC Genome Browser, <https://genome.ucsc.edu>
UniProt, <http://www.uniprot.org/>

References

1. Ishida, A., Asano, H., Hasegawa, M., Koseki, H., Ono, T., Yoshida, M.C., Taniguchi, M., and Kanno, M. (1993). Cloning and chromosome mapping of the human Mel-18 gene which encodes a DNA-binding protein with a new ‘RING-finger’ motif. *Gene* 129, 249–255.
2. Guo, W.-J., Datta, S., Band, V., and Dimri, G.P. (2007). Mel-18, a polycomb group protein, regulates cell proliferation and senescence via transcriptional repression of Bmi-1 and c-Myc oncoproteins. *Mol. Biol. Cell* 18, 536–546.
3. de Napoles, M., Mermoud, J.E., Wakao, R., Tang, Y.A., Endoh, M., Appanah, R., Nesterova, T.B., Silva, J., Otte, A.P., Vidal, M., et al. (2004). Polycomb group proteins Ring1A/B link ubiquitylation of histone H2A to heritable gene silencing and X inactivation. *Dev. Cell* 7, 663–676.

4. Akasaka, T., Kanno, M., Balling, R., Mieza, M.A., Taniguchi, M., and Koseki, H. (1996). A role for mel-18, a Polycomb group-related vertebrate gene, during the anterior-posterior specification of the axial skeleton. *Development* *122*, 1513–1522.
5. Morey, L., Santanach, A., Blanco, E., Aloia, L., Nora, E.P., Bruneau, B.G., and Di Croce, L. (2015). Polycomb Regulates Mesoderm Cell Fate-Specification in Embryonic Stem Cells through Activation and Repression Mechanisms. *Cell Stem Cell* *17*, 300–315.
6. Kajiume, T., Ninomiya, Y., Ishihara, H., Kanno, R., and Kanno, M. (2004). Polycomb group gene mel-18 modulates the self-renewal activity and cell cycle status of hematopoietic stem cells. *Exp. Hematol.* *32*, 571–578.
7. Kanno, M., Hasegawa, M., Ishida, A., Isono, K., and Taniguchi, M. (1995). mel-18, a Polycomb group-related mammalian gene, encodes a transcriptional negative regulator with tumor suppressive activity. *EMBO J.* *14*, 5672–5678.
8. Guo, W.-J., Zeng, M.-S., Yadav, A., Song, L.-B., Guo, B.-H., Band, V., and Dimri, G.P. (2007). Mel-18 acts as a tumor suppressor by repressing Bmi-1 expression and down-regulating Akt activity in breast cancer cells. *Cancer Res.* *67*, 5083–5089.
9. Jung, J.-H., Choi, H.-J., Maeng, Y.-S., Choi, J.-Y., Kim, M., Kwon, J.-Y., Park, Y.-W., Kim, Y.-M., Hwang, D., and Kwon, Y.-G. (2010). Mel-18, a mammalian Polycomb gene, regulates angiogenic gene expression of endothelial cells. *Biochem. Biophys. Res. Commun.* *400*, 523–530.
10. Park, J.H., Lee, J.Y., Shin, D.H., Jang, K.S., Kim, H.J., and Kong, G. (2011). Loss of Mel-18 induces tumor angiogenesis through enhancing the activity and expression of HIF-1 α mediated by the PTEN/PI3K/Akt pathway. *Oncogene* *30*, 4578–4589.
11. Uhlén, M., Fagerberg, L., Hallström, B.M., Lindskog, C., Oksvold, P., Mardinoglu, A., Sivertsson, Å., Kampf, C., Sjöstedt, E., Asplund, A., et al. (2015). Proteomics. Tissue-based map of the human proteome. *Science* *347*, 1260419.
12. Aloia, L., Di Stefano, B., and Di Croce, L. (2013). Polycomb complexes in stem cells and embryonic development. *Development* *140*, 2525–2534.
13. Aranda, S., Mas, G., and Di Croce, L. (2015). Regulation of gene transcription by Polycomb proteins. *Sci. Adv.* *1*, e1500737.
14. Wang, H., Wang, L., Erdjument-Bromage, H., Vidal, M., Tempst, P., Jones, R.S., and Zhang, Y. (2004). Role of histone H2A ubiquitination in Polycomb silencing. *Nature* *431*, 873–878.
15. Gao, Z., Zhang, J., Bonasio, R., Strino, F., Sawai, A., Parisi, F., Kluger, Y., and Reinberg, D. (2012). PCGF homologs, CBX proteins, and RYBP define functionally distinct PRC1 family complexes. *Mol. Cell* *45*, 344–356.
16. Srivastava, A., McGrath, B., and Bielas, S.L. (2017). Histone H2A Monoubiquitination in Neurodevelopmental Disorders. *Trends Genet.* *33*, 566–578.
17. Awad, S., Al-Dosari, M.S., Al-Yacoub, N., Colak, D., Salih, M.A., Alkuraya, F.S., and Poizat, C. (2013). Mutation in PHC1 implicates chromatin remodeling in primary microcephaly pathogenesis. *Hum. Mol. Genet.* *22*, 2200–2213.
18. Beunders, G., Voorhoeve, E., Golzio, C., Pardo, L.M., Rosenfeld, J.A., Talkowski, M.E., Simoncic, I., Lionel, A.C., Vergult, S., Pyatt, R.E., et al. (2013). Exonic deletions in *AUTS2* cause a syndromic form of intellectual disability and suggest a critical role for the C terminus. *Am. J. Hum. Genet.* *92*, 210–220.
19. Pierce, S.B., Stewart, M.D., Gulsuner, S., Walsh, T., Dhall, A., McClellan, J.M., Klevit, R.E., and King, M.-C. (2018). De novo mutation in *RING1* with epigenetic effects on neurodevelopment. *Proc. Natl. Acad. Sci. USA* *115*, 1558–1563.
20. Hoischen, A., van Bon, B.W.M., Rodríguez-Santiago, B., Gilissen, C., Vissers, L.E.L.M., de Vries, P., Janssen, I., van Lier, B., Hastings, R., Smithson, S.F., et al. (2011). De novo nonsense mutations in *ASXL1* cause Bohring-Opitz syndrome. *Nat. Genet.* *43*, 729–731.
21. Shashi, V., Pena, L.D.M., Kim, K., Burton, B., Hempel, M., Schoch, K., Walkiewicz, M., McLaughlin, H.M., Cho, M., Stong, N., et al.; Undiagnosed Diseases Network (2016). De Novo Truncating Variants in *ASXL2* Are Associated with a Unique and Recognizable Clinical Phenotype. *Am. J. Hum. Genet.* *99*, 991–999.
22. Bainbridge, M.N., Hu, H., Muzny, D.M., Musante, L., Lupski, J.R., Graham, B.H., Chen, W., Gripp, K.W., Jenny, K., Wienker, T.F., et al. (2013). De novo truncating mutations in *ASXL3* are associated with a novel clinical phenotype with similarities to Bohring-Opitz syndrome. *Genome Med.* *5*, 11.
23. Deciphering Developmental Disorders Study (2015). Large-scale discovery of novel genetic causes of developmental disorders. *Nature* *519*, 223–228.
24. Sobreira, N., Schiettecatte, F., Valle, D., and Hamosh, A. (2015). GeneMatcher: A Matching Tool for Connecting Investigators with an Interest in the Same Gene. *Hum. Mutat.* <https://doi.org/10.1002/humu.22844>.
25. Kramer, R.S.S., Jenkins, R., and Burton, A.M. (2017). InterFace: A software package for face image warping, averaging, and principal components analysis. *Behav. Res. Methods* *49*, 2002–2011.
26. Li, Z., Cao, R., Wang, M., Myers, M.P., Zhang, Y., and Xu, R.-M. (2006). Structure of a Bmi-1-Ring1B polycomb group ubiquitin ligase complex. *J. Biol. Chem.* *281*, 20643–20649.
27. McGinty, R.K., Henrici, R.C., and Tan, S. (2014). Crystal structure of the PRC1 ubiquitylation module bound to the nucleosome. *Nature* *514*, 591–596.
28. Jacob, J., Duchohier, H., and Cafiso, D.S. (1999). The role of proline and glycine in determining the backbone flexibility of a channel-forming peptide. *Biophys. J.* *76*, 1367–1376.
29. Tokuriki, N., and Tawfik, D.S. (2009). Stability effects of mutations and protein evolvability. *Curr. Opin. Struct. Biol.* *19*, 596–604.
30. Taherbhoy, A.M., Huang, O.W., and Cochran, A.G. (2015). BMI1-RING1B is an autoinhibited RING E3 ubiquitin ligase. *Nat. Commun.* *6*, 7621.
31. Lelieveld, S.H., Wiel, L., Venselaar, H., Pfundt, R., Vriend, G., Veltman, J.A., Brunner, H.G., Vissers, L.E.L.M., and Gilissen, C. (2017). Spatial Clustering of de Novo Missense Mutations Identifies Candidate Neurodevelopmental Disorder-Associated Genes. *Am. J. Hum. Genet.* *101*, 478–484.
32. Lek, M., Karczewski, K.J., Minikel, E.V., Samocha, K.E., Banks, E., Fennell, T., O'Donnell-Luria, A.H., Ware, J.S., Hill, A.J., Cummings, B.B., et al.; Exome Aggregation Consortium (2016). Analysis of protein-coding genetic variation in 60,706 humans. *Nature* *536*, 285–291.
33. Adler, P.N., Martin, E.C., Charlton, J., and Jones, K. (1991). Phenotypic consequences and genetic interactions of a null mutation in the *Drosophila* Posterior Sex Combs gene. *Dev. Genet.* *12*, 349–361.
34. Chun, T., Rho, S.B., Byun, H.-J., Lee, J.-Y., and Kong, G. (2005). The polycomb group gene product Mel-18 interacts with cyclin D2 and modulates its activity. *FEBS Lett.* *579*, 5275–5280.

35. Rivière, J.-B., Mirzaa, G.M., O’Roak, B.J., Beddaoui, M., Alcantara, D., Conway, R.L., St-Onge, J., Schwartzenuber, J.A., Gripp, K.W., Nikkel, S.M., et al.; Finding of Rare Disease Genes (FORGE) Canada Consortium (2012). De novo germline and postzygotic mutations in *AKT3*, *PIK3R2* and *PIK3CA* cause a spectrum of related megalencephaly syndromes. *Nat. Genet.* *44*, 934–940.
36. Mirzaa, G., Parry, D.A., Fry, A.E., Giamanco, K.A., Schwartzenuber, J., Vanstone, M., Logan, C.V., Roberts, N., Johnson, C.A., Singh, S., et al.; FORGE Canada Consortium (2014). De novo *CCND2* mutations leading to stabilization of cyclin D2 cause megalencephaly-polymicrogyria-polydactyly-hydrocephalus syndrome. *Nat. Genet.* *46*, 510–515.
37. Stutterd, C.A., and Leventer, R.J. (2014). Polymicrogyria: a common and heterogeneous malformation of cortical development. *Am. J. Med. Genet. C. Semin. Med. Genet.* *166C*, 227–239.
38. Lu, Y.-W., Li, J., and Guo, W.-J. (2010). Expression and clinicopathological significance of Mel-18 and Bmi-1 mRNA in gastric carcinoma. *J. Exp. Clin. Cancer Res.* *29*, 143.
39. Tao, J., Liu, Y.-L., Zhang, G., Ma, Y.-Y., Cui, B.-B., and Yang, Y.-M. (2014). Expression and clinicopathological significance of Mel-18 mRNA in colorectal cancer. *Tumour Biol.* *35*, 9619–9625.
40. Won, H.-Y., Lee, J.-Y., Shin, D.-H., Park, J.-H., Nam, J.-S., Kim, H.-C., and Kong, G. (2012). Loss of Mel-18 enhances breast cancer stem cell activity and tumorigenicity through activating Notch signaling mediated by the Wnt/TCF pathway. *FASEB J.* *26*, 5002–5013.

Supplemental Data

Missense Mutations of the Pro65 Residue of PCGF2 Cause a Recognizable Syndrome Associated with Craniofacial, Neurological, Cardiovascular, and Skeletal Features

Peter D. Turnpenny, Michael J. Wright, Melissa Sloman, Richard Caswell, Anthony J. van Essen, Erica Gerkes, Rolph Pfundt, Susan M. White, Nava Shaul-Lotan, Lori Carpenter, G. Bradley Schaefer, Alan Fryer, A. Micheil Innes, Kirsten P. Forbes, Wendy K. Chung, Heather McLaughlin, Lindsay B. Henderson, Amy E. Roberts, Karen E. Heath, Beatriz Paumard-Hernández, Blanca Gener, the DDD study, Katherine A. Fawcett, Romana Gjergja-Juraški, Daniela T. Pilz, and Andrew E. Fry

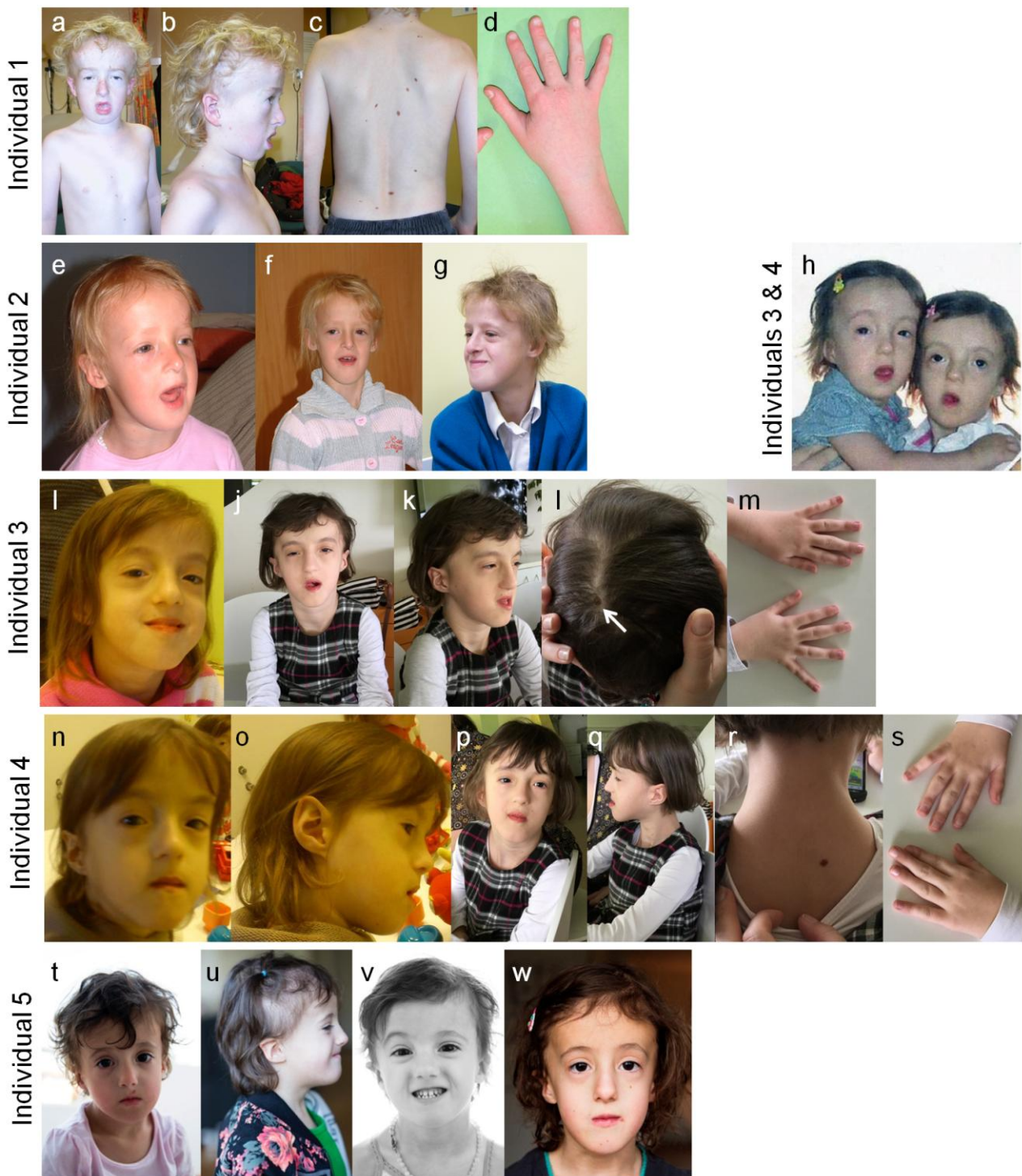


Figure S1. Additional images of individuals (1-5) with pathogenic *PCGF2* mutations. Images are clustered for each individual. Each cluster is marked with the number which corresponds to the one used in the manuscript. The images show: individual 1 (male) at 12 years (a-d); individual 2 (female) at 4.5 years (e), 8.5 years (f) and 13 years (g); individuals 3 and 4 (female) at 2 years (h); individual 3 at 4 years (i) and 8 years (j-m); individual 4 at 4 years (n,o) and 8 years (p-s); individual 5 (female) at 4 years (t-v) and 7 years (w). Consistent facial features include a high, broad forehead; long face; malar hypoplasia; small mouth and palpebral fissures; a prominent nose (particularly in older individuals); and dysplastic, low-set ears. Individual 1, the oldest in the group, had multiple pigmented macules on his trunk (c). Similar macules were seen on the scalp of individual 3 (white arrow, l) and the neck of individual 4 (r).

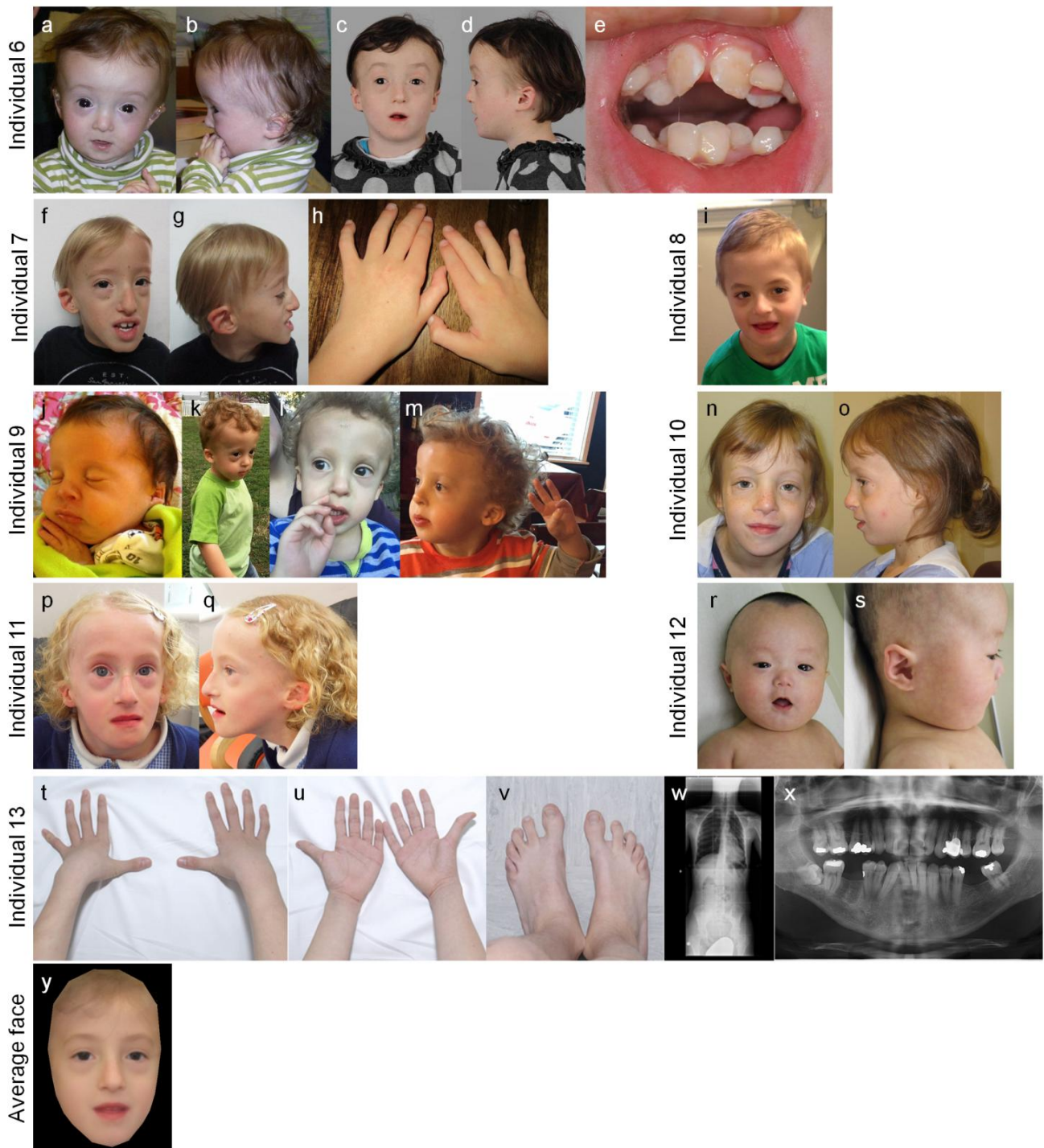


Figure S2. Additional images of individuals (6-12) with pathogenic *PCGF2* mutations. Images are clustered for each individual. Each cluster is marked with the number which corresponds to the one used in the manuscript. The images show: individual 6 (male) at 1 year (a,b) and 9 years (c-e); individual 7 (male) at 7 years (f-h); individual 8 (male) at 6 years (i); individual 9 (male) at 1 month (j), 2 years (k,l) and 3 years (m); individual 10 (female) at 9 years (n,o); individual 11 (female) at 8 years (p,q); individual 12 (male) at 3 months (r,s); individual 13 (male) at 11 years (t-v). Radiological images from individual 13 show a long narrow thorax with mild scoliosis (w) and radicular resorption of secondary teeth (x). Minor digital anomalies with mild 5th finger clinodactyly and tapering fingers are shown (h,t,u).The composite average face (y) was generated from images of nine unrelated individuals (1-3, 5-8, 10 and 11).

Supplemental Note: Case Reports

Individual 1

This 21-year-old male is the eldest of 3 siblings of unrelated white British parents. He was born at term weighing 2900g (9th centile). His mother had taken mefloquine anti-malarial prophylaxis in the first 6 weeks of pregnancy. Postnatally he fed poorly and was hypotonic. Dysmorphic features were noted and his occipitofrontal circumference (OFC) was 90th centile by the age of 1 year. He sat at 12 months and walked at 4 years. He developed conductive hearing impairment and chronic, severe constipation which improved slowly during childhood. He drooled constantly and underwent successful submandibular duct realignment surgery. Over time he remained small (growth centile at age 11 years were: height 1st and weight 5th) but with relative macrocephaly (OFC ~97th centile). He was last evaluated at 21 years of age. His speech remains unintelligible, although his receptive language has improved and he demonstrates an eagerness to learn. He has a flat facial profile, thin hair, satyr ears, a narrow nose, and a number of pigmented nevi on his torso. A brain MRI at 16 months showed dilatation of the 3rd and 4th ventricles and thinning of the corpus callosum. There was a generalised reduction in the white matter but myelination was normal. A skeletal survey at 2.5 years revealed a gibbus deformity due to hypoplasia of L1 vertebra, delayed epiphyseal ossification, particularly of the carpal bones, and pseudo-epiphyses of many metacarpals. A recent echocardiogram showed dilation of the aorta at the sinus of Valsalva (diameter 4.7cm, Z score ~7.7). Extensive metabolic and genetic testing was normal. Microarray comparative genomic hybridization (array-CGH) analysis identified duplications of 0.4Mb at Xp21.2 and 0.5Mb at Xp21.1-p11.4, both inherited from his unaffected maternal grandfather. The DDD Study also identified maternally inherited

variants of uncertain significance in the *USP9X* and *PHF8* genes (classified using the ACMG guidelines).

Individual 2

This 15-year-old female is the elder of two sisters. She was born at 42 weeks gestation after an uneventful pregnancy, birth weight 3340g (25th-50th centile). She fed poorly and failed to thrive. At 6 months her growth centiles were: weight 0.4th, length 25-50th, OFC 25th. Her feeding slowly improved and by late childhood her growth centiles were: weight 9th, height 50-75th, OFC 0.4th. Developmentally, she rolled at 9 months, sat and crawled at 12 months, and walked at 2 years, at which time she demonstrated speech delay with a vocabulary of approximately 15 single words. Initially in mainstream school, she was moved to a unit with learning support, where she has made some progress. Severe chronic constipation was eventually managed successfully by an antegrade colonic enema procedure performed at 12 years of age. Individual 2 was last evaluated at 15 years of age. She has moderate intellectual disability with specific speech and language problems, and mild conductive hearing loss which required grommets. Clinical examination revealed frontal bossing with malar hypoplasia, a prominent nasal tip, small mouth, and short sternum with widely spaced nipples. She has bitemporal balding with generally sparse hair, but normal skin, nails and teeth. Her palpebral fissures are short and down-slanting, and she has a long face with a highly arched palate and prognathism, which has gradually become more prominent with age. She has long narrow hands and fingers. Cardiac MRI showed a normal aortic root at the sinus of Valsalva (2.5cm, Z score 0.29), mild aortic valve regurgitation, and mild dilatation of the left ventricle. This examination incidentally identified a Morgagni hernia of the diaphragm. Array-CGH, cranial MRI and EEG, were all reported to be normal.

Individual 3

This 8-year-old female is twin 1 of monozygotic twins (see Individual 4). They were the first live-born children to non-consanguineous parents. The pregnancy was complicated by polyhydramnios. Birth was at term, weight 2050g (<0.4th centile), length 45cm (1st centile), Apgar scores good. She suffered a grade 2 intraventricular/periventricular haemorrhage and a patent ductus arteriosus (PDA) was surgically closed at 2 months of age. At 21 months her length and weight were on the 5th centile, OFC 5th-10th centile. Both twins were noted to have speech delay, dysmorphic features, increased limb tone with axial hypotonia, and mild choreoathetotic movements of the hands. This twin sat at 1 year and walked at 3 years. At age 5 years 3 months her height was on the 25-50th centile. She was noted to be hyperactive and her language, motor skills, and understanding, were poor but improving. She had large adenoids and severe obstructive sleep apnea. Following adenoidectomy she continued open-mouth breathing. She had frequent, recurrent respiratory infections. Most recently evaluated at 8.5 years of age, she had poor expressive speech, coordination difficulties, constipation, mild diplegia, and features of attention deficit hyperactivity disorder. She had no history of seizures and an EEG was normal. Brain MRI at 21 months of age showed relatively symmetric, multifocal T2 hyperintensities within the deep white matter, most prominent around atria of the lateral ventricles where the changes were confluent. The lateral ventricles were slightly enlarged and some perivascular spaces were mildly prominent. There was extensive, bilateral polymicrogyria affecting the perisylvian regions, inferior frontal, parietal, temporal and superior occipital lobes. MR angiogram (MRA) showed tortuosity of the internal carotid arteries. Routine karyotype, subtelomeric MLPA and array-CGH were normal.

Individual 4

This 8-year-old female is twin 2 of monozygotic twins (see Individual 3). As for twin 1, her Apgar scores were good, and birth weight was 2090g (<0.4th centile), length 44cm (1st centile). She also suffered a grade 2 intraventricular/periventricular haemorrhage, and a PDA closed spontaneously. At 21 months length and weight were on the 5th centile, OFC 5th-10th centile. This twin sat at 1 year and walked at 2.5 years. At 3 years she was noted to have a small left-sided diaphragmatic Morgagni hernia, found incidentally following a foreign body aspiration, and surgically corrected. She had gastroesophageal reflux which improved following the hernia repair. At age 5 years 3 months her height was between the 75th and 91st centile. She was noted to be hyperactive and her language, motor skills, and understanding, were still poor but improving. She had large adenoids and severe obstructive sleep apnea. Following adenoidectomy she continued open-mouth breathing. She had frequent, recurrent respiratory infections. Most recently evaluated at 8.5 years of age, she had poor expressive speech, coordination difficulties, constipation, mild diplegia, and features of attention deficit hyperactivity disorder. She had no history of seizures and an EEG was normal. Brain MRI at 21 months of age showed relatively symmetrical, multifocal T2 hyperintensities within the deep white matter, with some early confluence. The lateral ventricles were slightly enlarged with some prominence of perivascular spaces, and extensive, bilateral polymicrogyria affected the perisylvian, inferior frontal, parietal and temporal regions. She did not have an MRA. Routine karyotype, subtelomeric MLPA and array-CGH were normal.

Individual 5

This 7-year-old female is the child of unrelated parents. Growth delay was noted after 20 weeks gestation and polyhydramnios developed at 28 weeks. Antenatal karyotype, array-CGH, and TORCH screen of amniotic fluid, were normal. Birth was induced at 38+2 weeks gestation, birth weight 2200g (~2nd centile), length 42 cm (<0.4th centile). Linear growth

caught up by 6 months of age but she remained underweight. At 3-4 months a blue coloured subcutaneous swelling was noted on the left side of her nose, diagnosed as a subcutaneous haemangioma or epidermal cyst. She initially bottle fed satisfactorily but suddenly stopped sucking at 8-9 months, was fed by nasogastric tube, and noted to be very hypotonic with clenched fists and adducted thumbs. Examination at 1.5 years of age revealed plagiocephaly with a flat occiput and large fontanelle (4cm x 4cm), sparse hair, triangular face with flat profile, downslanting eyebrows with synophrys and medial flare, and long eyelashes. She had upslanting palpebral fissures, epicanthic folds, a broad nasal tip, small dysplastic ears with triangular conchae, small lobes, narrow ear canals, and absent crus on the smaller left ear. She has a small mouth, smooth philtrum, high-arched palate and bifid uvula. She had a 5mm nevus at the left knee and diffuse hypertrichosis of the lumbar area. Developmentally, she smiled at 11 months, walked from 2 years, and spoke her first words at 3 years, following which she made progress and can use full sentences at 7 years of age. Moderate conductive hearing impairment, partly due to otitis media, was treated with grommets and hearing aids, which improved her speech. At 3.6 years a SON-R intelligence test showed a performance IQ of 75, and although the verbal scale IQ was 101, her speech is slow compared to her peers. She used to wake frequently at night and pulled the hair of other children. At 7 years of age she has progressed in her motor and speech development but tonal dysregulation and some coordination problems remain. She has chronic constipation, her hair remains sparse, she has a convergent squint, hypermetropia and astigmatism, and small, widely spaced teeth; her height is normal but weight low. Brain MRI at age 3 years 4 months showed relatively symmetric, multifocal T2 hyperintensities within the deep white matter, most prominent around atria of lateral ventricles, where changes showed early confluence. There were prominent perivascular spaces. The lateral and 4th ventricles were slightly enlarged, but no evidence of obstructive hydrocephalus. There was a tiny focus of haemosiderin in the right

caudo-thalamic groove. An MRA showed tortuosity of internal carotid arteries. Echocardiography showed a small atrial septum defect (ASD) with left-right shunt, mild dilatation of the ascending aorta which later resolved, mitral and tricuspid valve prolapse, and a PDA, which was surgically closed. Renal and liver ultrasound scans were normal. Spinal X-rays showed the body of her T3 vertebra was small. Postnatal array-CGH found a *de novo* duplication of 15q11.2 (238kb) with no genes in the region.

Individual 6

This 15-year-old female is the eldest of three children born to unrelated parents. Intrauterine growth restriction (IUGR) was noted at 20 weeks gestation and she was born at 37+3 weeks, weight 1652g (<0.4th centile). In infancy she had central hypotonia but was peripherally hypertonic, which later resolved. Developmental milestones were globally delayed and she first walked on her 3rd birthday. She had severe gastroesophageal reflux and constipation. She remained very small but has responded to growth hormone, commenced age 7 years. She had conductive hearing impairment treated with grommets. Significant obstructive sleep apnea was diagnosed aged 10 years, not resolved by adenotonsillectomy. Menarche occurred at 11 years. At age 12 years she attended both mainstream and special schools, and had an anxiety disorder with some autistic behaviours. She has mild sensorineural hearing impairment, but compliance with aids is poor. Her vision is normal. She has persistent constipation and both bladder and bowel incontinence of uncertain cause. She has metatarsus adductus, planovalgus feet, and prominent interphalangeal joints. A skeletal survey showed tall vertebrae with mild scoliosis and thoracic kyphosis, slender bones, coxa valga, and a truncated sacrum with flexion deformity at S4 and only three sacral segments. Brain MRI at age 5 years 4 months showed relatively symmetric, multifocal T2 hyperintensities within the deep and subcortical white matter bilaterally, with early confluence in some deeper regions.

Prominent perivascular spaces, together with a cavum septum pellucidum and verge were observed. There was subtle bilateral perisylvian polymicrogyria, more prominent on the left, and a left cerebral parietal developmental venous anomaly. Compared to MR imaging four years previously, appearances were stable. Echocardiogram found an ASD which closed spontaneously. Metabolic and array-CGH testing were normal.

Individual 7

This 10-year-old male was born at 38 weeks gestation after a pregnancy complicated by polyhydramnios, mild fetal hydronephrosis, and IUGR, birth weight 2380g (1st centile). He fed poorly in the neonatal period requiring an NG tube. He had hypotonia, plagiocephaly, transient corneal opacities, and dysmorphic features including low-set ears, pectus excavatum and torticollis. He was treated for gastroesophageal reflux. He suffered frequent recurrent respiratory infections and febrile episodes in his preschool years, undergoing adenoidectomy and grommet insertion aged 2 years. This helped his feeding but mild hearing impairment remained. Ophthalmic examination revealed anisometropia, mild tortuosity of the retinal vasculature, and concave optic discs. Occasional nocturnal seizures started prior to age 2 years but responded to lamotrigine treatment. He developed a sleep disorder which responded to melatonin and clonazepam. He had global developmental delay, uttering his first words by 2 years, and started walking at 5 years with splints. At 7 years of age he had hypotonia, failure to thrive (height and weight <3rd centile), and could only walk and climb stairs unsteadily with splints. He is dysarthric but has a good vocabulary and is sociable. His skin is fair and hair sparse. The plagiocephaly persists and his face is flat with prognathism. He has mild blepharophimosis, dysplastic ear helices, a high palate, pectus excavatum, and normal hands, feet, and genitalia (the left testicle is small). Echocardiogram found a large ASD and small PDA, which were both closed by percutaneous catheterization at 1 year.

Renal ultrasound showed transient, moderate bilateral hydronephrosis. Brain MRI at age 10 months showed a few scattered deep white matter T2 hyperintensities, together with mild prominence of the lateral ventricles. Array-CGH was normal.

Individual 8

This 9-year-old male was born at 40+3 weeks gestation after a pregnancy complicated by polyhydramnios, birth weight 3200g (25th-50th centile). At birth he was noted to have small, low-set, crumpled ears, and torticollis. In infancy he had hypotonia and delayed developmental milestones, and sat independently at 11 months. He had significant gastroesophageal reflux exacerbated by multiple food allergies, oral tactile sensory sensitivity, and chronic constipation. He was diagnosed with exotropia at 13 months which ultimately required bilateral surgical repair. He has global developmental delay and autistic spectrum disorder with stereotypical movements, occasional self-injurious stimulatory behaviours, and disrupted sleep. He is nonverbal and communicates with signs, gestures, and tablet applications. At 6.5 years he was found to have a right thoracolumbar neuromuscular scoliosis (but normal spine MRI) that has improved without intervention. He has had several episodes of metabolic acidosis and hypoglycaemia with mild dehydration, cause unknown. Sequential brain MRI has shown stable non-specific patchy areas of T2 prolongation in the periventricular white matter. Brain MRI at age 3.1 years showed relatively symmetric, multifocal T2 hyperintensities within the deep white matter bilaterally, most marked around atria of lateral ventricles. There were prominent perivascular spaces, including within the corpus callosum. An MRA showed tortuous vessels, most prominently the carotid and vertebral arteries. Echocardiogram at 13 months of age demonstrated mild-moderate dilatation of the aortic root and ascending aorta, which has persisted. Further surveillance has shown stable dolichoectasia of the carotid, vertebra-basilar, posterior cerebral, and anterior

cerebral arteries. Routine karyotype, array-CGH and a range of genetic investigations were normal.

Individual 9

This 5-year-old male was born at 39+4 weeks gestation following an uncomplicated pregnancy and delivery, birth weight 2812g (>9th<25th centile). He had hypotonia in the neonatal period but a reasonable suck. He had global developmental delay from infancy, particularly in speech and language, and sat independently from 15 months. He underwent unilateral orchidopexy for an undescended testis. He has mild relative macrocephaly and dysmorphic facial features including a triangular appearance to his lower face, a high-arched palate, abnormal pinnae with truncated upper helices, telecanthus with shortened palpebral fissures, infra-orbital hypoplasia, and a significantly recessed mid-face. He had a prominent pectus carinatum. Brain MRI revealed enlarged extra-axial spaces, irregular gyral pattern and mild cerebellar vermis hypoplasia. Ultrasound imaging of the heart, kidneys, and hips were normal. Routine karyotype and array-CGH were normal.

Individual 10

This 8-year-old female was born at 39 weeks gestation following an uncomplicated pregnancy. birth weight 1928g (<0.4th centile). She had hypotonia in the neonatal period and dysmorphic features were noted, including posteriorly-rotated ears, hypertelorism, a flat nasal bridge, and pectus excavatum. She had persistent growth problems, with height and weight consistently less than 3rd centile, and relative macrocephaly (OFC ~75th centile). She had recurrent respiratory syncytial virus infections and multiple episodes of otitis media, requiring myringotomy and adenoidectomy. She walked at 18-24 months, began talking

around 2.5 years with significant articulation problems. She had hypotonia, global developmental delay, educational difficulties, and achieved toilet training at 6 years. She had a single seizure associated with a urinary tract infection, and an episode of supraventricular tachycardia associated with a near syncopal event. Echocardiogram showed a mildly dilated ascending aorta (Z score 2.97). Brain MRI at age 13 months showed scattered, multifocal deep white matter T2 hyperintensities and a thin corpus callosum. There was mild lateral ventriculomegaly, with coarctation of the frontal horns. Renal ultrasound revealed a duplex collecting system requiring surgical repair. Her karyotype and array-CGH were normal.

Individual 11

This 9-year-old female was the second child of unrelated parents. The pregnancy was complicated by intrauterine growth restriction, increased nuchal translucency and echogenic bowel. Amniocentesis showed a normal karyotype. She was delivered by caesarean section at 38 weeks gestation, birth weight 2440g (~5th centile). She required mechanical ventilation from which she was slow to wean due to episodes of hypoventilation. She had a suspected seizure in the newborn period but there was no recurrence. She sat independently at 13 months. She had significant feeding difficulties and severe constipation for the first two years. Initially tube-fed, she progressed to the bottle, then developed severe gastroesophageal reflux, and consequently poor weight gain. At 21 months growth centiles were: length 9th centile, weight 2nd centile, OFC 50th centile. The feeding problems slowly improved through childhood and the constipation improved with medical management. She has astigmatism and delayed language skills, including phonics, but is conversational. Her hearing is satisfactory. She attends a mainstream school with one-to-one support. At school she performs approximately 3 years behind her chronological age. She is sociable but lacks stranger awareness, has a short attention span, and is becoming stubborn. Her height has

varied between the 9th and 25th centiles, with OFC consistently >50th centile. Her hair is thin and slow growing, especially in the temporal regions. Her dysmorphic features include plagiocephaly, low set dysplastic ears, long face, asymmetric cry, prominent nose, protruding columella, thin upper lip, and small teeth in her lower jaw. She appeared to have bilateral adducted thumbs when young with in-curved 3rd and 4th toes. MRI brain at 11 weeks was reported to be normal. She had a normal echocardiogram. Routine karyotype, subtelomeric screen, array-CGH, myotonic dystrophy, *SMN1* and *SHOC2* testing, were all normal. Her mother, who was intellectually normal and not dysmorphic but had slightly sparse scalp hair, was mosaic for the *PCGF2* mutation (approximately 21% in blood DNA).

Individual 12

This 3-year-old male is the child of non-consanguineous parents. The pregnancy was uneventful and he was a normal birth at 39 weeks gestation following induction of labour weight 2820g (10th centile). His length was 46cm (3rd centile) and OFC 35.0cm (50th centile). He had an apneic spell at 5 minutes post-delivery and was subsequently noted to have central hypotonia, feeding difficulties and cryptorchidism, for which he later underwent bilateral orchidopexy. Significant feeding and vomiting persisted in early infancy but he was otherwise healthy, and growth parameters were maintained. He had dysmorphic features including redundant neck skin, small satyr ears, small upturned nose, brachycephaly and a flat facial profile. At 9 months he was globally delayed with persistent hypotonia, and weight fell to the 3rd centile. He walked unsteadily at 29 months, with some improvement by 36 months. At 30 months his OFC was 51cm (50th centile). At 3 years he is still non-verbal but showing progress with social interactions, though anxious. Feeding problems persist but he is managed orally. Brain MRI at age 2.5 years showed relatively symmetric, multifocal T2 hyperintensities within the deep white matter bilaterally, most marked around atria of lateral

ventricles, features which were not evident on initial imaging at 10 months. Bilateral perisylvian polymicrogyria was present. A cavum septum pellucidum was noted, with absence of the midsection of the septum. Array-CGH identified a paternally inherited 1.22Mb duplication at 1q44. Extensive metabolic investigations, and tests for Prader-Willi syndrome and myotonic dystrophy, were normal.

Individual 13

This 18-year-old male is the first child of unrelated parents. He was born at 40 weeks gestation following an uncomplicated pregnancy, birth weight 3250g (25th centile). Developmental delay was noted from 8 months of age and at 9 months his growth centiles were: weight 1st, length 3rd, OFC 25th-50th. He had difficulty feeding and frequent vomiting in the first 18 months of life, and first walked at 26 months. He had learning and social skill difficulties, including difficulties in writing and language skills, but a good visual memory. He repeated a school year at age 7 years. He had facial hypotonia and drooled at the age of 12 years. At 13 years 5 months his growth centiles were: weight 9th-25th, height 75th, OFC 50th-75th. At 16 years his growth centiles were: weight 9th-25th, height 25th-50th. He continues to have difficulties with pronunciation and is hard to understand. He smiles normally but it is difficult to interpret his emotions. He is impulsive and avoids contact with sand or grass when barefoot. He has fine and gross motor clumsiness but no history of seizures. On examination he has sparse hair, small ear lobes, wide forehead, triangular face, prominent nose, facial hypotonia with dribbling, and a high arched palate. He has long, narrow fingers and toes, bilateral 2nd to 5th finger camptodactyly, and mild pes cavus. He has a long, narrow thorax with kyphoscoliosis. He has dental malposition with radicular resorption of secondary teeth. Brain MRI at age 8 years was reported to be normal. A bone age at 5 years 7 months was delayed. Echocardiography has identified slowly progressive

dilation of the aorta, currently treated with beta blockers. Routine karyotype, array-CGH, metabolic testing, *FBNI* and *DMPK* testing, and a NGS panel of 35 genes related to aortic syndromes, were all normal. Permission to publish clinical photographs was not granted.